Metallurgy and materials
Metalurgia e materiais

Texture evolution in the Fe-30.5Mn-8.0Al-1.2C and Fe-30.5Mn-2.1Al-1.2C steels upon cold rolling

http://dx.doi.org/10.1590/0370-44672015690122

Fabrício Mendes Souza
Dr. Professor
PEB - Secretaria de Estado de Educação
de Minas Gerais
Belo Horizonte – Minas Gerais – Brasil
souzafm@yahoo.com.br

Angelo Fernando Padilha
Dr.–Ing. Professor
Universidade de São Paulo - USP
Escola Politécnica da Universidade de São Paulo
Departamento de Engenharia
Metalúrgica e de Materiais
São Paulo – São Paulo – Brasil
padilha@usp.br

Ivan Gutierrez-Urruti
Senior Researcher
National Institute for Materials Science
Research Center for Strategic Materials
Microstructure Design Group
Japan - Tsukuba
gutierrezurrutia.ivan@nims.go.jp

Dierk Raabe
Director
Max-Planck-Institut fur Eisenforschung GmbH
Department of Microstructure Physics
and Alloy Design
Dusseldorf – Germany
d.raabe@mpie.de

Abstract

Crystallographic textures of the austenitic low-density Fe-30.5Mn-8.0Al-1.2C (8Al) and Fe-30.5Mn-2.1Al-1.2C (2Al) (wt.%) steels were examined during cold rolling by means of electron backscatter diffraction (EBSD) and electron channeling contrast imaging (ECCI). Random oriented grains orient towards Goss- and brass-components along the α-fiber as the strain increased, with activation of slip, mechanical twinning, and shear banding, for both steels. S- and copper-orientations were also observed in the 8Al steel at 50% reduction. The route of Cu-CuT-Goss-brass texture evolution was found in the 2Al alloy. Cu, Goss, and brass textures occur as a dominant texture in the deformed 8Al alloy. Copper-type texture accompanied with slip at low reduction (20%), as well as Cu-type shear bands, and shear banding inside Goss-oriented grains at higher reduction (50%), were observed in the 8Al steel. It is suggested that this copper-type rolling texture may be attributed to the Al addition, which contributes to its low twinning activity compared to that in the 2Al alloy. Cu-CuT-brass f.c.c. rolling texture transition to form the Brass-type texture was observed at higher reduction in the 2Al alloy with strong similarity to that found in other Fe-Mn-C system TWIP steels.

Keywords: austenitic steels; Fe-Mn-C alloys; Fe-Mn-Al-C alloys; texture; EBSD; TWIP steels.

1. Introduction

Austenitic high manganese lightweight steels are useful materials for structural application purposes in the automobile industry, owing to their good combinations of strength and ductility (GRÄSSEL *et al*, 2000). The Fe-30.5Mn-2.1Al-1.2C (wt.%) (2Al) and Fe-30.5Mn-8.0Al-1.2C (8Al) alloys have medium and high Stacking Fault Energy, SFE, respectively (SOUZA *et al*, 2015). The crystallographic texture evolution in deformed TWIP steels of the Fe-Mn-C system has been largely studied (BOUAZIZ *et al*, 2011; DE COOMAN *et al*, 2011; GAZDER *et al*, 2011; BRACKE *et al*, 2009). It is well known that the alloy-type texture has practically only the brass component, while for the pure metal-type, the copper, S, and brass components are about equally strong. These two texture types were observed in Ni-40%Co alloy as a texture transition from pure metal-type to alloy-type, as a function of Co-content, owing to twinning activation over and above normal slip. Furthermore, the texture transition in such alloy presented quite similar texture changes as a function of the amount of cold rolling (RAY, 1995). The activation of both slip and mechanical twinning has been associated to the brass-type cold rolling texture formation, which is commonly observed in the TWIP steels (VERCAMMEN *et al*, 2004; BRACKE *et al*, 2009; LÜ *et al*, 2011;

HAASE *et al*, 2013). Textures of the 8Al and 2Al alloys remain not studied under cold rolling condition up to now. The aim of this work is to analyze the crystallographic texture evolution, correlating to the activated deformation mechanisms with progressing strain and corresponding to some already studied cold-rolled Fe-Mn-C alloys. Distinct textures can be examined in these 8Al and 2Al steels, owing to their different SFE's. We performed a detailed characterization of the texture evolution and deformation mechanisms in the cold-rolled 8Al and 2Al steels by using electron backscatter diffraction (EBSD) and electron channeling contrast imaging (ECCI).

2. Experimental

The chemical compositions of the steels were Fe-30.5Mn-8.0Al-1.2C and Fe-30.5Mn-2.1Al-1.2C (wt. %). Details on alloy processing and mechanical behavior can be found in (SPRINGER and RAABE, 2012; GUTIERREZ-URRUTIA and RAABE, 2013). The steels were cold rolled up to 50% thickness reduction (Fig. 2), strain level (ε) up to 0.69, because the maximum force of the used laboratory rolling mill was not sufficient to further reduce the thickness of the specimens. Macrotextures of the cold rolled materials were determined by electron backscatter diffraction (EBSD) technique with step size of 5 μm from different regions on the specimens (with surface area of about 70 mm^2), reaching scanned total area of about 8 mm^2 in size for each sample. High resolution Kikuchi pattern images were scanned with step size of about 0.1 μm for microtexture analysis. The EBSD measurements were performed by a 6500 F JEOL field emission gun scanning electron microscope (FEG-SEM) equipped with a TSL OIM EBSD software system. EBSD scans were carried out on the specimen plane surface parallel to the rolling direction (RD) and normal direction (ND). The microscope was operated at 15 kV acceleration voltage and 15 mm working distance. Kikuchi pattern image quality (IQ) maps, inverse pole figures (IPF) maps, and Kernel average misorientation (KAM) maps were obtained by means of TSL-OIM software calculation. The microstructure and microtexture in specimens of the 8Al steel was characterized by using the electron channeling contrast imaging (ECCI) technique combined with EBSD. This approach has been successfully applied to the characterization of dislocation and twin substructures in high-Mn steels. ECCI observations were carried out in a Zeiss Crossbeam instrument (XB 1540, Carl Zeiss SMT AG, Germany). The developed EBSD-based set-up was used to obtain ECCI images. Detailed conditions can be found in (GUTIERREZ-URRUTIA and RAABE, 2009, 2013).

3. Results

Deformation texture in fcc metals is commonly interpreted in terms of the stacking fault energy (SFE). High-SFE metals, such as Al, Cu and Ni, which deform by dislocation slip at room temperature, develop the so-called pure metal Copper-type texture. This texture is characterized by a strong β-fibre with an increasing intensity from the brass component, through to the S and then Cu texture components (HÖLSCHER *et al*, 1994; ENGLER and HIRSCH, 2002; HUMPHREYS and HATHERLY, 2004). Low-SFE alloys, such as Cu-Zn, typically deform by deformation twinning, and develop the so-called alloy or Brass-type texture. This texture builds up a α-fibre with a lower intensity on the Cu component, and higher on the brass and Goss components (HIRSCH *et al*, 1988; LEFFERS and RAY, 2009). In Fig. 1 can be seen the EBSD color coded map (inverse pole figure (IPF) map) for the hot-rolled and cold-rolled 8Al and 2Al steels with reductions up to 50%, illustrating the orientation of the grains and their distributions in the microstructure. The grains become gradually elongated along the rolling direction (RD) and oriented towards to brass- and Goss-orientations (green color) as the cold rolling degree increases.

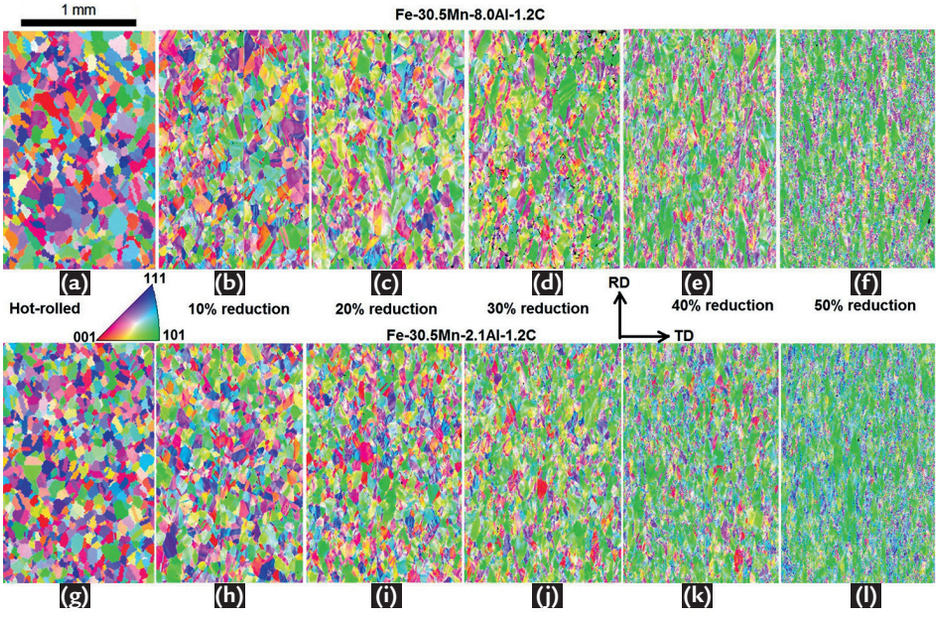

Figure 1
EBSD inverse pole figure maps illustrating the orientation and the distribution of the grains for the hot-rolled and cold-rolled (10-50% thickness reduction) 8Al and 2Al steels. RD: rolling direction and TD: transversal direction.

The texture evolution in the deformed samples is shown in Figs. 2 and 3 by means of orientation distribution functions (ODFs), on the φ_2=45, φ_2=65, and φ_2=90 sections, and intensities of the α, β, and τ fibers, as well as texture components of the hot-rolled and cold-rolled (with ε up to 0.69) 8Al and 2Al steels, respectively. The hot-rolled materials exhibited a weak texture mainly formed by C and B components. The deformation texture of the 8Al steel is characterized by a Cu-type texture and strong G component (Fig. 2). The texture of this steel developed at 40% reduction. Intensities of the Cu, S, G, and B components increased with strain. The Cu component is developed at strains greater than 0.36, where the intensities of the G and B components are greater, whereas those of the Cu and S components are lesser. The intensities on the G and B components increased with strains greater than 0.36, and G saturated at 0.69 with an intensity of f(g)=8, while B saturated at 0.51 with f(g)=6. Intensities of the B and G increased gradually with strain. B component intensity (f(g)=6) is lesser than that of G (f(g)=8) while Cu component intensity increased to 6 times random at strain of 0.69 (Fig. 2). The deformation texture of the 2Al steel is characterized by a Brass-type texture, and strong G component (f(g)=9) at ε=0.69 (Fig. 3). G and B components are developed at strains higher than 0.36. This deformation texture has been found in FeMnC (BRACKE *et al*, 2009; LÜ *et al*, 2011; HAASE *et al*, 2013) and FeMnAlSi (VERCAMMEN *et al*, 2004) high-Mn steels. B component intensity (f(g)=8) is smaller than that of G, as well as Cu texture component changed to CuT at strain of 0.69 (Fig. 3).

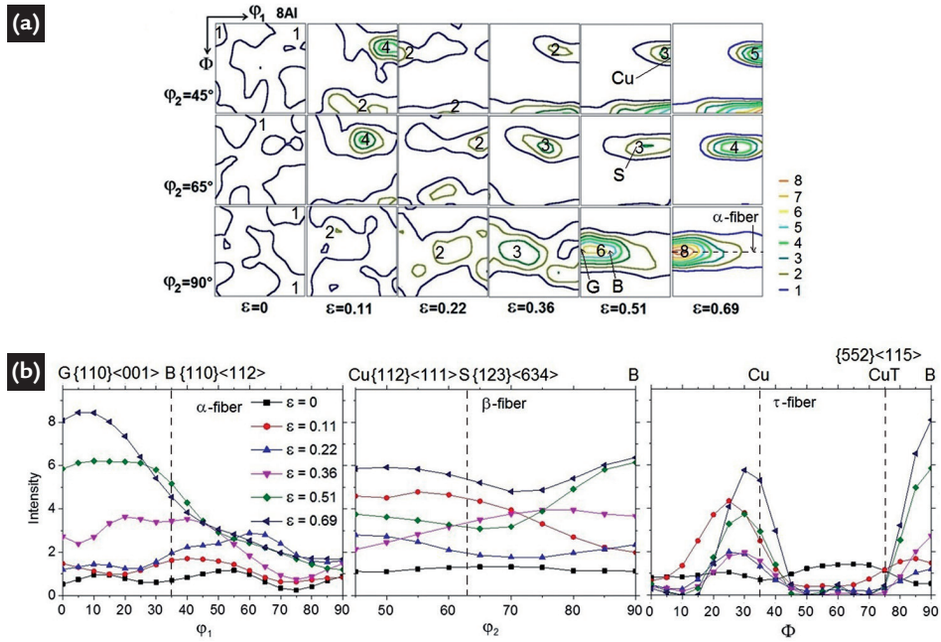

Figure 2
(a) Evolution of the orientation distribution functions (ODFs) on the φ2=45, φ2=65, and φ2=90 sections. (b) Intensities of the α, β, and τ fibers and texture components of the 8Al steel with progressing deformation.

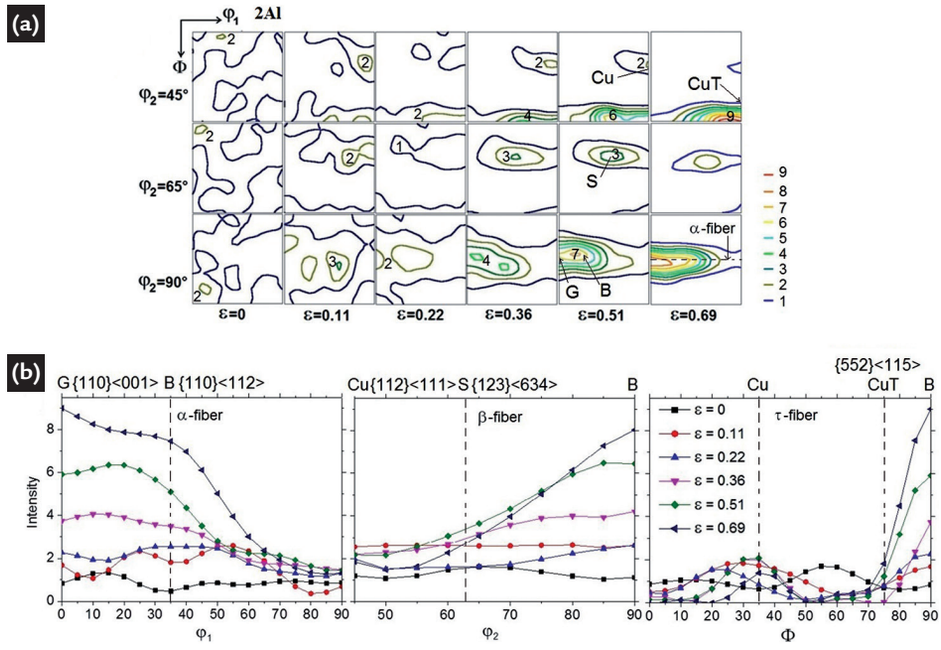

Figure 3
(a) Evolution of the orientation distribution functions (ODFs) on the φ2=45, φ2=65, and φ2=90 sections. (b) Intensities of the α, β, and τ fibers and texture components of the 2Al steel with progressing deformation.

4. Discussion

In the 8Al steel deformation twins were not observed at low strain (< 0.22), indicating that occurrence of the S and Cu orientations accompanies slip in both steels, as also found in the Fe-22Mn-0.4C steel (LÜ *et al*, 2010). In

Fig. 4(a) and (b) can be seen IQ maps of the microstructures at strain levels of 0.51 and 0.69, respectively, with the inverse pole figure maps from Cu- and G–oriented regions within 15°, for the 8Al steel. Their respective ODFs are also shown. The dependence of deformation twinning on the initial grain orientation is influenced by grain rotation, due to slip, and by the Schmid factor (YANG *et al*, 2006). Despite the dominance of slip, twins were also observed in grains with orientations close to Cu component in this steel at higher strains (Fig. 4a). It has been reported that the Schmid factor ratio is μ=μt/μs, where μt is the Schmid factor for twinning, and μs that for slip for the relevant twin and slip systems, since the highest value of μ (1.16) is attributed to selectively occurrence of twins in Cu oriented grains (HIRSCH *et al*, 1988). This probably also contributed to the Cu-type rolling texture development (see Fig. 2) in the 8Al alloy at high deformation level. Mechanical twins and shear bands (SB) were found in Cu-oriented and G-oriented grains, where a bundle of twins inside shear bands (Fig. 4) were also observed, by means of EBSD. In order to clarify the texture behavior and activation of deformation mechanisms at strain level of 0.69 in the 8Al steel, ECCI images (Fig. 5(b) and (c)) were obtained from brass-oriented and a Goss-oriented grains, which are shown from IPF map (Fig. 5(a)). Fig. 5 shows that the occurrence of these orientations accompanies the activation of stacking faults, planar dislocation structures, mechanical twins, and shear bands. Goss-component grains, specially has shear banding with many deformation twins. These microtexture features are well-established as the retainment of G texture in the shear bands (see also Fig. 4b), just as is also found in other f.c.c. alloys (HIRSCH *et al*, 1988; DONADILLE *et al*, 1989; SALEH *et al*, 2011). In previous work (SOUZA *et al*, 2015) it was reported that strong mechanical twinning formed in the 2Al steel at higher strain (~0.7). This accompanied the formation of G, and B texture components (Fig. 3). This is in agreement with the microstructure and rolling texture observed in other high-Mn austenitic steels (VERCAMMEN *et al*, 2004; BRACKE *et al*, 2009; LÜ *et al*, 2011; HAASE *et al*, 2013), where mechanical twinning occurs mainly in B-oriented grains at medium strain levels.

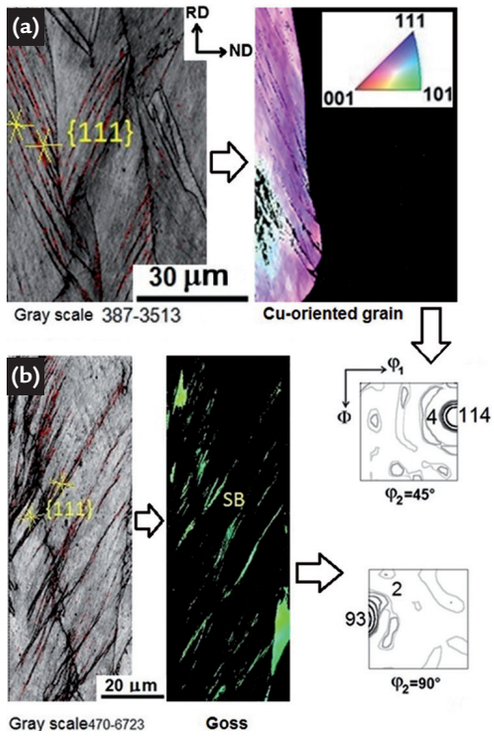

Figure 4
(a) IQ map of the microstructure and the inverse pole figure (IPF) map from a Cu--oriented grain within 15° in the 8Al steel at 40% thickness reduction.
(b) IQ map of the microstructure with the IPF map from the G–oriented regions within 15° in the 8Al steel at 50% thickness reduction. The red lines indicate the Σ3 twin boundaries, and the black lines denote the high angle grain boundaries. {111} plane traces are indicated close to SB. The respective orientation distribution functions (ODFs), with minimum and maximum intensities, for the relevant highlighted orientations, are also presented.

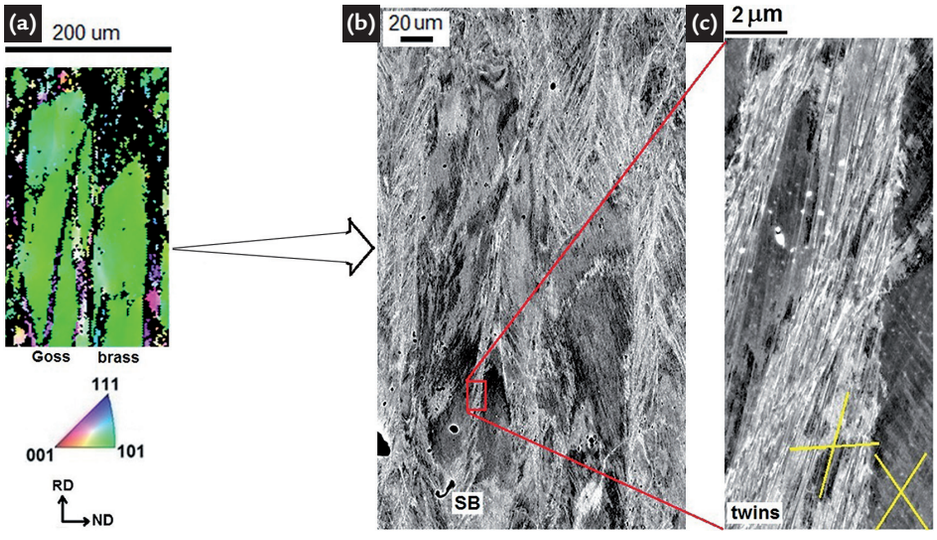

Figure 5
(a) Inverse pole figure maps from the Goss- and brass-oriented grains,
(b) ECCI image of this same region, and
(c) ECCI enlarged area from a SB, in the 8Al steel at 50% thickness reduction, showing strong mechanical twinning inside SB. X-like marks are {111} plane traces.

In the 2Al steel, Cu texture component transforms to CuT component at strain of 0.69 as shown in Fig. 3. This texture behavior has frequently been referred to as twinning of the transformed Cu orientation into the CuT orientation, which slips to G and/or B texture components (deviation from Cu-type texture to B-type texture). This texture transition was associated to an overshooting/latent-hardening effect caused by the closely spaced twin lamellae. Pronounced effect of latent hardening develops texture components with {111} approximately parallel to the RD. When this effect is caused by the twin lamellae, the onset of shear banding can occur (LEFFERS and RAY, 2009; BRACKE *et al*, 2009; LÜ *et al*, 2011; HAASE *et al*, 2013). As a result, orientation densities on the G and B components increased along the α-fiber in the 2Al steel at higher strain levels (Fig. 3). Nevertheless, deviation from Cu-type texture to B-type texture (LEFFERS and RAY, 2009) was not observed in the 8Al steel with high-SFE, owing to its high amount of Al added as alloying element, since the twin formation is reduced, as the critical resolved shear stress required for twin formation increases with increasing SFE (PARK *et al*, 2010; HONG *et al*, 2012). The texture transition from Cu-type to B-type was also observed when twinning became an additional important mode of deformation in Ni-40%Co alloy in different deformation stages in the α-brass and MP35N alloys (ASGARI *et al*, 1997). The 2Al alloy, with profuse mechanical twinning activity, has this rolling texture route of Cu-CuT-B-G (B-type), probably due to the occurrence of the different deformation stages as investigated in such tensile-deformed alloy in previous work (GUTIERREZ-URRUTIA and RAABE, 2012). On the other hand, the 8Al alloy has strong Cu, S, and brass components (Cu-type), probably due to the suppressed mechanical twinning. G orientation dominant texture component forms preferentially in non-crystallographic shear bands (usually oriented at 25-35° to the RD) and in matrix, has been observed in some f.c.c. alloys (DONADILLE *et al*, 1989; HUMPHREYS and HATHERLY, 2004; LI *et al*, 2008; SALEH *et al*, 2011). Accordingly, G component appeared with highest intensity in the 2Al steel (Fig. 3) and in the 8Al steel (Fig. 2) at ε=0.69, where shear banding was activated (Fig. 5) (SOUZA *et al*, 2015). In summary, the 8Al steel at reduction ranged in 10%-40% has Cu, G, and B components with f(g)=6 and at 50% G component increases to f(g)=8, while the 2Al steel at reduction ranged in 10%-40% has G and B components with about f(g)=6 and G component with f(g)=9 and B with f(g)=8 at 50%.

5. Conclusions

Crystallographic texture evolution was examined in the two cold rolled low-density high-Mn steels, namely, Fe-30.5Mn-2.1Al-1.2C and Fe-30.5Mn-8.0Al-1.2C (wt%). Macrotexture results showed that grains oriented towards the Goss- and brass-components along the α-fiber, with activation of slip, mechanical twinning, and shear banding, for both steels cold rolled up to strain of 0.69. S- and copper-orientations were also observed in the deformed 8Al steel at such strain. The route of Cu-CuT-G-B texture evolution, seen in other alloys, was found in the 2Al alloy, while Cu, G and B texture formed as a dominant texture in the 8Al alloy, with contribution of deformation twinning. Detailed microtexture features, such as copper-type texture accompanied with slip at low strain and Cu-type shear bands were also observed in the 8Al steel, as well as, shear banding (SB) inside Goss-oriented grains. The f.c.c. rolling texture transition that contributed to the Brass-type texture formation in the 2Al steel was observed at ε~0.7. It was suggested that Al addition can be attributed to the texture transition from brass-type to copper-type, which increases the Fe-Mn-Al-C system alloy SFE in alloys with higher amount of Al (~8wt%). The cold rolling texture of the 2Al steel was close to that found in TWIP steels belonging to the Fe-Mn-C system.

6. Acknowledgments

The authors acknowledge the financial support by the Science without Borders, Brazil's scholarship program, for the CNPq postdoctoral fellowship (process number: 237863/2012-0), and by the German Research Foundation in the framework of the SFB 761 – steel ab initio.

7. References

ASGARI, S., EL-DANAF, E., KALIDINDI, S. R., DOHERTY, R. D. Strain hardening regimes and microstructural evolution during large strain compression of low stacking fault energy fcc alloys that form deformation twins. ***Metallurgical and Materials Transactions A***. v. 28A, 1781-1795, 1997.

BRACKE, L., VERBEKEN, K., KESTENS, L., PENNING, J. Microstructure and texture evolution during cold rolling and annealing of a high Mn TWIP steel. ***Acta Materialia***. v. 57, p. 1512–1524, 2009.

BOUAZIZ, O., ALLAIN, S., SCOTT, C.P., CUGY, P., BARBIER, D. High manganese austenitic twinning induced plasticity steels: A review of the microstructure properties relationships. ***Current Opinion in Solid State and Materials Science***. v. 15, p. 141-168, 2011.

DONADILLE, C., VALLE, R., DERVIN, P., PENELLE, R. Development of texture and microstructure during cold-rolling and annealing of f.c.c. alloys: example of an austenitic stainless steel. ***Acta Metallurgica et Materialia***. v. 37, p. 1547-1571, 1989.

DE COOMAN, B. C., CHIN, K.-G., KIM, J. High Mn TWIP Steels for Automotive Applications. ***New Trends and Developments in Automotive System Engineering.*** p. 101-128, 2011.

ENGLER O., HIRSCH J. Texture control by thermomechanical processing of AA-6xxx Al–Mg–Si sheet alloys for automotive applications – a review. ***Materials Science and Engineering A***. v. 336, p. 249–262, 2002.

GAZDER, A. A., SALEH, A. A., PERELOMA, E. V. Microtexture analysis of cold--rolled and annealed twinning-induced plasticity steel. ***Scripta Materialia***. v. 65, p. 560-563, 2011.

GRÄSSEL, O., KRÜGER, L., FROMMEYER, G., MEYER, L. W. High strength Fe-Mn-(Al, Si) TRIP/TWIP steels development – properties – application. ***International Journal Plasticity.*** v. 16, p. 1391-1409, 2000.

GUTIERREZ-URRUTIA, I., RAABE, D. Multistage strain hardening through dislocation substructure and twinning in a high strength and ductile weight-reduced Fe–Mn–Al–C steel. ***Acta Materialia***. v. 60, p. 5791–5802, 2012.

GUTIERREZ-URRUTIA, I., RAABE, D. Influence of Al content and precipitation state on the mechanical behavior of austenitic high-Mn low-density steels. ***Scripta Materialia***. v. 68, p. 343-47, 2013.

GUTIERREZ-URRUTIA, I., RAABE, D. Dislocation density measurement by electron channeling contrast imaging in a scanning electron microscope. ***Scripta Materialia.*** v. 66, p. 343-346, 2012.

GUTIERREZ-URRUTIA, I., ZAEFFERER, S., RAABE, D. Electron channeling contrast imaging of twins and dislocations in twinning-induced plasticity steels under controlled diffraction conditions in a scanning electron microscope. ***Scripta Materialia***. v. 61, p. 737–740, 2009.

HAASE, C., CHOWDHURY, S. G., BARRALES-MORA, L. A., MOLODOV, D. A., GOTTSTEIN, G. On the Relation of Microstructure and Texture Evolution in an Austenitic Fe-28Mn-0.28C TWIP Steel During Cold Rolling. ***Metalurgical and Materials Transactions A.*** v. 44A, p. 911-922, 2013.

HIRSCH, J., LÜCKE, K., HATHERLY, M.. Overview No. 76: Mechanism of deformation and development of rolling textures in polycrystalline f.c.c. Metals-III. The influence of slip inhomogeneities and twinning. ***Acta Metallurgica***. v. 36, p. 2905-2927, 1988.

HÖLSCHER, M., RAABE, D., LÜCKE, K. Relationship between rolling textures and shear textures in f.c.c. and b.c.c. metals. ***Acta Metallurgica et Materialia***. v. 42, p. 879-886, 1994.

HONG, S., SHIN, S. Y., KIM, H. S., LEE, S., KIM, S.-K., CHIN, K.-G., KIM, N. J. Effects of Aluminum Addition on Tensile and Cup Forming Properties of Three Twinning Induced Plasticity Steels. ***Metallurgical and Materials Transactions A.*** v. 43, pp. 1870-1883, 2012.

HUMPHREYS, F. J., HATHERLY, M.. ***Recrystallization and related annealing phenomena***. (2nd. Ed.) Oxford: Pergamon, 2004. p. 67-89.

LEFFERS, T., RAY, R. K. The brass-type texture and its deviation from the copper--type texture, ***Progress in Materials Science.*** v. 54, p. 351-396, 2009.

LI, H., YIN, F., SAWAGUCHI, T., OGAWA, K., ZHAO, X., TSUZAKI, K. Texture evolution analysis of warm-rolled Fe-28Mn-6Si-5Cr shape memory alloy. ***Materials Science and Engineering A.*** v. 494, p. 217-226, 2008.

LÜ, Y., HUTCHINSON, B., MOLODOV, D. A. GOTTSTEIN G. Effect of deformation and annealing on the formation and reversion of e-martensite in an Fe–Mn–C alloy. ***Acta Materialia.*** v. 58, p. 3079-3090, 2010.

LÜ, Y., MODOLOV, D. A., GOTTSTEIN, G. Correlation Between Microstructure and Texture Development in a Cold-rolled TWIP Steel. ***ISIJ International.*** v. 51, p. 812–817, 2011.

PARK, K.-T. Tensile deformation of low-density Fe–Mn–Al–C austenitic steels at ambient temperature. ***Scripta Materialia***. 2012, http://dx.doi.org/10.1016/j.scriptamat.2012.09.031.

PARK, K.-T., JIN, K. G., HAN, S. H., HWANG S. W., CHOI K., LEE C. S. Stacking fault energy and plastic deformation of fully austenitic high manganese steels: Effect of Al addition. ***Materials Science and Engineering A.*** v. 527, p. 3651-3661, 2010.

RAY, R. K. Rolling textures of pure nickel, nickel-iron and nickel-cobalt alloys. ***Acta Metallurgica et Materialia***. v. 43, p. 3861-3872, 1995.

SALEH, A. A., PERELOMA, E. V., GAZDER A. A. Texture evolution of cold rolled and annealed Fe–24Mn–3Al–2Si–1Ni–0.06C TWIP steel. ***Materials Science and Engineering A.*** v. 528, pp. 4537-4549, 2011.

SOUZA, F. M., PADILHA, A. F., GUTIERREZ-URRUTIA, I., RAABE, D. Microstructural analysis in the Fe-30.5Mn-8.0Al-1.2C and Fe-30.5Mn-2.1Al-1.2C steels upon cold rolling. ***REM - Revista Escola de Minas.*** v. xx, p. xx, 2015. (submitted for publication).

SPRINGER, H., RAABE D. Rapid alloy prototyping: Compositional and thermo-mechanical high throughput bulk combinatorial design of structural materials based on the example of 30Mn-1.2C-xAl triplex steels. ***Acta Materialia.*** v. 60, p. 4950–4959, 2012.

VERCAMMEN, S., BLANPAIN, B., DE COOMAN, B.C., WOLLANTS, P. Cold rolling behaviour of an austenitic Fe–30Mn–3Al–3Si TWIP-steel: the importance of deformation twinning. ***Acta Materialia.*** v. 52, p. 2005–2012, 2004.

YANG, P., XIE, Q., MENG, L., DING, H., TANG, Z. Dependence of deformation twinning on grain orientation in a high manganese steel. ***Scripta Materialia.*** v. 55, p. 629-631, 2006.

Received: 24 July 2015 - Accepted: 13 January 2016.